Xi'an Shiyou Daxue Xuebao (Ziran Kexue Ban)/
Journal of Xi'an Shiyou University, Natural Sciences Edition
ISSN: 1673-064X
E-Publication: Online Open Access
Vol: 68 Issue 03 | 2025
DOI: 10.5281/zenodo.15112737

THREE-DIMENSIONAL NUMERICAL STUDY OF AERODYNAMIC PERFORMANCE ENHANCEMENT AROUND A SPIROID WINGLET

ZINEB HEMMAMI*
Electromechanic Department, Institut of Maintenance and Industrial Safety, University of Mohammed Ben Ahmed - Oran2, Oran, Algeria. *Corresponding Author Email: zinebhemmami@gmail.com

AZZEDDINE HAMMAMI
Mechanical Engineering Department, University of Science and Technology of Oran Mohammed Boudiaf, Oran, Algeria.

Abstract

This study investigates the aerodynamic performance enhancement of a spiroid winglet utilizing the NACA 2412 airfoil through three-dimensional numerical simulations. Winglets are a well-established technology for improving the aerodynamic efficiency of aircraft wings by reducing induced drag. However, conventional winglet designs can still experience significant vortex shedding and flow separation, limiting their efficacy. The spiroid winglet geometry, inspired by the theoretical minimum induced drag shape, shows promise in mitigating these issues. Computational fluid dynamics (CFD) analyses were conducted using a finite volume method to solve the Reynolds-Averaged Navier-Stokes equations coupled with a Shear Stress Transport turbulence model. The wing-winglet model incorporated a spiroid winglet design based on the NACA 2412 airfoil. Simulations were performed at angles of attack ranging from 0° to 25° to assess the winglet's performance over the operational envelope. Results demonstrate that the spiroid winglet configuration significantly reduces induced drag compared to the baseline wing without a winglet, with drag reductions of up to 23.8% at the design cruise condition of 2° angle of attack. Furthermore, the wingtip vortices are found to be more diffuse with lower peak vorticity magnitudes, indicating mitigation of strong tip vortex formation. The spiroid winglet delays flow separation up to higher angles of attack compared to conventional winglets. Detailed flow visualizations and surface pressure distributions elucidate the fluid dynamic mechanisms behind the performance gains. Overall, the numerical study validates the merits of spiroid winglets and provides insights for optimizing future aerodynamic designs.

Keywords: Spiroid Winglet, Aerodynamic, Drag, Lift, CFD, Finite Volume.

INTRODUCTION

Aircraft designers are continually pursuing innovative aerodynamic solutions to improve efficiency and reduce fuel consumption. Among these solutions, winglets have emerged as an effective technology for minimizing induced drag, a major contributing factor to overall drag on aircraft wings. Conventional winglet designs, while beneficial, can still experience significant vortex shedding and flow separation, limiting their full potential [1]. This has motivated researchers to explore unconventional winglet geometries inspired by theoretical minimum induced drag shapes, such as the spiroid winglet.

The spiroid winglet concept, first proposed by Whitcomb [2], exhibits a curved planform shape that gradually decreases in sweep angle towards the tip, mimicking the ideal non-planar lifting surface for minimizing induced drag [3]. Numerous computational and experimental studies have demonstrated the merits of spiroid winglets in reducing wing-induced drag and associated wingtip vortices compared to conventional designs [1-4].

ISSN: 1673-064X
E-Publication: Online Open Access
Vol: 68 Issue 03 | 2025
DOI: 10.5281/zenodo.15112737

Guerrero et al. [1] highlighted how the spiroid geometry facilitates more diffuse wingtip vortices with lower peak vorticity magnitudes, thereby mitigating strong tip vortex formation.

In addition to drag reduction, spiroid winglets have shown promise in delaying flow separation to higher angles of attack relative to conventional winglets [5]. This characteristic is particularly advantageous for improving aerodynamic performance across the operational envelope, including high angles of attack encountered during takeoff and landing.

The selection of an appropriate airfoil profile is crucial for optimizing the spiroid winglet design. The NACA 2412 airfoil has gained interest due to its favorable aerodynamic characteristics at low Reynolds numbers [4], relevant to the flow regime around winglets. Takenaka et al. [4] investigated the aerodynamic performance of the NACA 2412 wing at low Reynolds numbers, providing insights into its behavior.

Several studies have explored the impact of winglets on wing performance. Najafian Ashraf and Sedaghat [6] investigated the use of winglets to improve lift coefficient and lift-to-drag ratio. In a broader analysis, Hui, Cheng, and Chen (2021) [7] reviewed the aerodynamic performance of various wingtip devices, including winglets and wingtip slots. Their review highlighted the potential of winglets to reduce induced drag, a key contributor to overall drag, but also acknowledged the ongoing research on optimizing winglet designs for different flight conditions.

Focusing specifically on spiroid winglets, Nicolosi et al. (2021) [8] conducted an aerodynamic efficiency study of modern spiroid winglet designs. Their findings suggest that spiroid winglets offer advantages over traditional straight winglets, particularly at cruise flight conditions. Suhail Mostafa1 et al [9] investigated spiroid winglets, exploring their theoretical significance and the process involved in selecting an optimal aerodynamic spiroid winglet configuration that yields efficient performance results. The primary focus is on enhancing the lift-to-drag ratio (L/D), reducing induced drag, and analyzing chordwise and spanwise pressure distributions, vorticity formation, and vortex strength. The study compares the aerodynamic performance of a simple wing, a wing with a conventional winglet, and a wing with the optimized spiroid winglet design by varying several geometric parameters. Detailed computational fluid dynamics (CFD) analyses are performed on each configuration under representative cruise conditions. The research presented in this paper demonstrates that the spiroid winglet exhibits superior performance compared to the other options in terms of vortex mitigation and overall drag reduction. Behrouz Fathi [10] numerically investigated the aerodynamics around a wind turbine blade equipped with a winglet using computational fluid dynamics (CFD) simulations. The objective is to apply a spiroid winglet design to examine the vortex effects at the tip of the "NREL offshore 5-MW baseline wind turbine" blade. While spiroid winglets have shown promise in other applications, they have not yet been widely adopted in the wind energy sector due to the excessive costs associated with their production relative to the potential benefits. This study explores a spiroid winglet configuration with

ISSN: 1673-064X
E-Publication: Online Open Access
Vol: 68 Issue 03 | 2025
DOI: 10.5281/zenodo.15112737

varying twist distributions and camber orientations pointing towards the suction side (downstream). Comparative analyses are conducted between two operating conditions, evaluating parameters such as pressure, thrust, torque, relative velocity, streamlines, vorticity, and ultimately, the mechanical power output. The findings aim to assess the viability and potential advantages of incorporating spiroid winglets into wind turbine blade designs for enhanced aerodynamic performance.

Karthick Dhileep et al [11] found that the rapid growth in global air travel driven by improving socio-economic conditions has not been matched by reductions in airline operating costs, with fuel expenses continuing to dominate at 27% of total expenses. Induced drag, caused by the pressure differential between the wings, is a major contributor, accounting for 25% of total drag during cruise and up to 60% during takeoff. To address this issue, endplates or winglets were introduced in the 1980s to mitigate wingtip vortices. Numerous studies have explored various winglet configurations, revealing that the angle at which winglets are inclined significantly influences the strength of the shed wingtip vortices. This research computationally investigates the effect of winglet eccentricity on aerodynamic performance by analyzing a baseline swept wing with vertical winglets and seven modified models featuring curved winglets with different eccentricities. These configurations are evaluated at various angles of attack and a Reynolds number of 4.0×10^6. The results demonstrate that the curved semi-spiroid winglet with an eccentricity of 0.2 outperforms the clean wing, exhibiting a 9.85% improvement in aerodynamic efficiency across the pre-stall angle of attack range.

This study aims to leverage the potential of spiroid winglets in conjunction with the NACA 2412 airfoil through three-dimensional numerical simulations. By combining these concepts, the research seeks to elucidate the fluid dynamic mechanisms behind the anticipated performance enhancement and contribute to the development of more efficient aerodynamic designs for aircraft wings.

In addition, This paper focuses on the aerodynamic performance of spiroid winglets. These winglets have a unique, curved design that may offer advantages over traditional straight winglets. By examining the existing research on winglets and spiroid designs, this paper aims to explore the potential for spiroid winglets to enhance the aerodynamic performance of wings.

Numerical Solution:

In this section, we will present the numerical approach that was carried out by a finite volume computation code. For mesh validation, we went through a series of refinements until the results stabilized. The mesh was created using a software, followed by validation of the computation code by comparing numerically obtained results with experimental results. Subsequently, we will present the results obtained. We were interested in the aerodynamic characteristics of the airfoil, namely the drag and lift coefficients, as well as the pressure and velocity distributions around the airfoil.

ISSN: 1673-064X
E-Publication: Online Open Access
Vol: 68 Issue 03 | 2025
DOI: 10.5281/zenodo.15112737

After comparing our results with experimental results, we obtain Figure-1- which shows the lift coefficient distribution Cp around a NACA 2412 airfoil.

This figure demonstrates that our numerical results are in good agreement with the experimental data, especially in the ranges (0 < α < 3) and (12 < α < 15) [12]. And is slightly underpredicted in the area between 3< α < 12

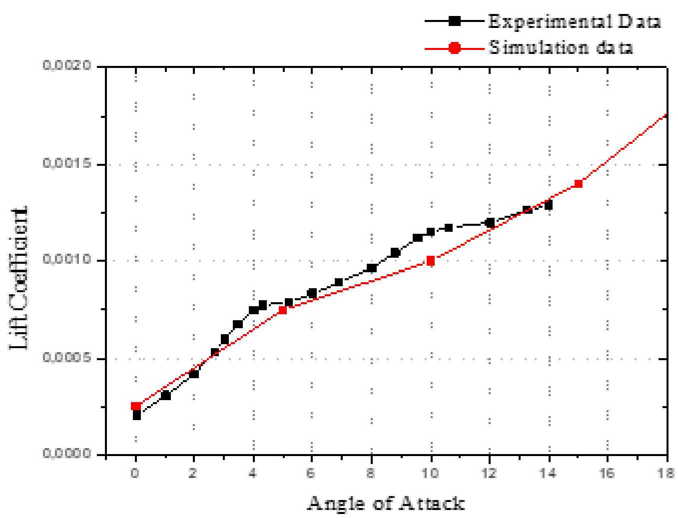

Fig 1: Comparison between experimental data and numerical results

In order to mesh the geometry to be usable by a code, the geometry created by Solidworks must be improved with the aim of obtaining a good mesh using a software to avoid calculation errors.

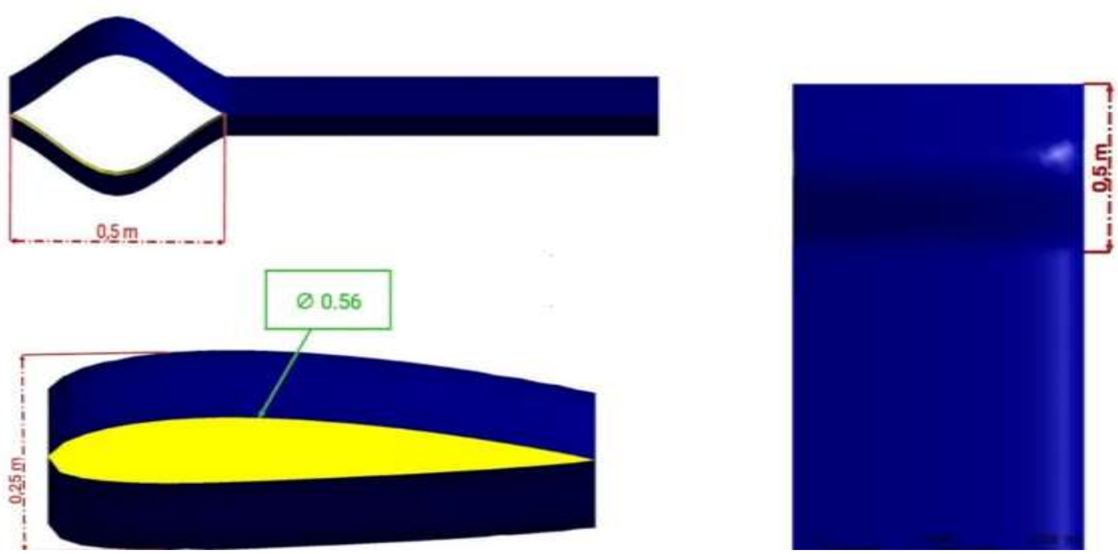

Fig 2: Spiroid Winglet Dimensions

ISSN: 1673-064X
E-Publication: Online Open Access
Vol: 68 Issue 03 | 2025
DOI: 10.5281/zenodo.15112737

A spiroid winglet features a curved planform shape that gradually decreases in sweep angle from the wing root towards the tip. Its geometry is inspired by the theoretical ideal of a non-planar lifting surface that produces minimum induced drag.

Unlike conventional winglets with a constant sweep angle (Fig-2-, the spiroid winglet's leading and trailing edges form continuous spiral curves. The spanwise reduction in sweep follows an approximately logarithmic relation, resulting in a tight inward spiral near the tip region.

This unique shape allows the spiroid to behave as a highly efficient extension of the wing's lifting surface. The winglet's airfoil sections are typically derived from established low-speed airfoils like the NACA 2412 series.

However, the sections get progressively twisted and cambered towards the tip to align with the local flow directions dictated by the spiroid's tight curvature as shown in fig-3-. By closely approximating the ideal lifting surface geometry, the spiroid winglet aims to minimize wingtip vortices and associated induced drag penalties.

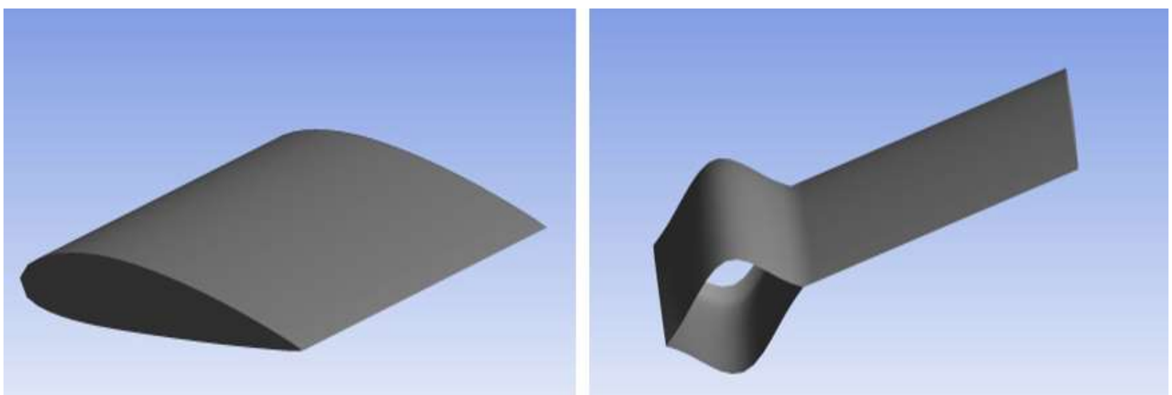

Fig 3: Naca Profile 2415 with and without Winglet

After creating the geometry, 4 volumes (meshing domains) are created from the winglet surfaces, and this is to facilitate the meshing and have the mesh more refined on the walls in order to obtain more precise results on the boundary layer. These 4 volumes allow us to have a simpler geometry than that of the winglets compared to the computational domain.

Figure 4 represents the final mesh of the block with the winglet, a hybrid mesh (hexahedral and tetrahedral) as shown in Figure 6. The domain is composed of 3,000,000 nodes.

Note that the cell density near the winglet surface is fine, and larger sized away from it. After examining the mesh elements, the boundary conditions must be defined by the software.

Xi'an Shiyou Daxue Xuebao (Ziran Kexue Ban)/
Journal of Xi'an Shiyou University, Natural Sciences Edition
ISSN: 1673-064X
E-Publication: Online Open Access
Vol: 68 Issue 03 | 2025
DOI: 10.5281/zenodo.15112737

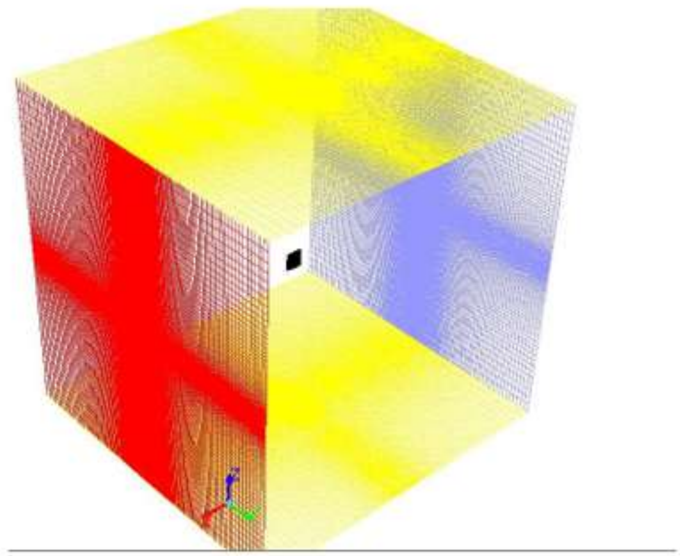

Fig 4: Computational domain

An inlet velocity initial condition is used to define the flow velocity at the inlet. The front face of the flow control volume is set as an initial condition for the inlet velocity. To specify the flow properties entering the computational volume or domain in addition to the front face, the left, top and bottom faces are also specified to ensure that the flow properties are properly taken into account by the FLUENT solver. The flow outlet plane is specified as an outflow condition. The winglet surface is specified as a "wall" boundary condition to differentiate the solid and liquid regions. Finally, the symmetry plane is specified as a symmetry plane. A summary of the boundary conditions used for this winglet is shown in Figure 5.

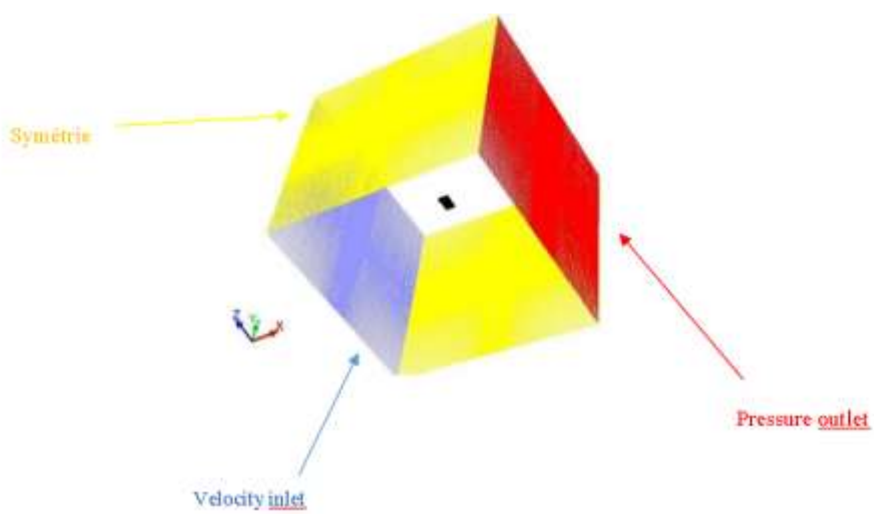

Fig 5: Boundary conditions

ISSN: 1673-064X
E-Publication: Online Open Access
Vol: 68 Issue 03 | 2025
DOI: 10.5281/zenodo.15112737

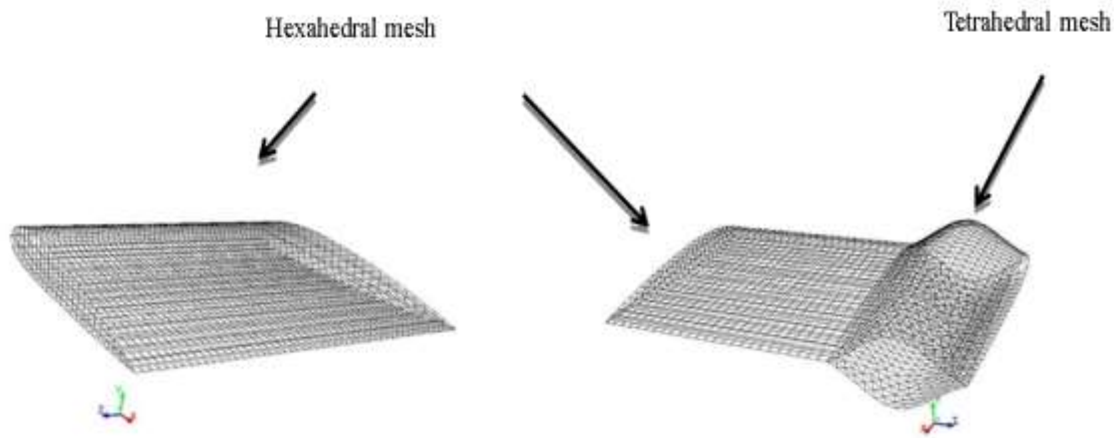

Fig 6: meshing types

The 'k-ω' turbulence model is used to solve the problem, as it is widely used based on the transport equations for turbulent kinetic energy and dissipation rate. It predicts consistent results especially for simple shear flows. However, it has a local and linear dependence of the Reynolds stresses on the mean field and it is not well suited for complex flows (recirculation, strong anisotropy, negative production, etc.).

The simulation is carried out under the following conditions:

$P_0 = 0$ Pa

T = 288.16K

V = 20 m/s

The air properties are as follows:

$\gamma = 1.4$

$\mu = 1.7894.10^{-5}$ kg.m^{-1}. s^{-1}

Expression for the Lift Force Fz

Lift is a force that depends on the pressures acting on the wing.

The entire wing span creates lift, so the lift will be proportional to the wing area.

The airfoil shape determines the quality of the lift. This shape is characterized by a coefficient named Cz.

The air through which the wing moves has characteristics dependent on other quantities such as temperature, pressure, etc. The overall parameter used is the density in kg/m^3.

This leads to the following expression:

Lift = Dynamic Pressure x Area x Airfoil Characteristics

$Fz = 1/2\ \rho V^2\ S\ Cz$

Xi'an Shiyou Daxue Xuebao (Ziran Kexue Ban)/
Journal of Xi'an Shiyou University, Natural Sciences Edition
ISSN: 1673-064X
E-Publication: Online Open Access
Vol: 68 Issue 03 | 2025
DOI: 10.5281/zenodo.15112737

Where: Fz is the lift force ρ is the air density V is the airspeed S is the wing area Cz is the lift coefficient dependent on the airfoil shape

Expression for Drag:

Drag depends, like lift, on the pressure acting on the wing, the wing area, and the airfoil characteristics. This leads to the following expression:

Drag = Dynamic Pressure x Area x Airfoil Characteristics

$Fx = 1/2\ \rho V^2\ S\ Cx$

Where:

ρ: Air density in kg/m^3

S: Wing area in m^2

V: Airspeed in m/s

Cx: Drag coefficient of the airfoil

So the drag force Fx is proportional to the dynamic pressure ($1/2\ \rho V^2$), the wing area S, and the drag coefficient Cx which characterizes the airfoil shape's drag properties.

Results and discussions:

The lift coefficients as well as the drag coefficients collected from the numerical simulation are compared by plotting them on the same graph for each coefficient.

Lift:

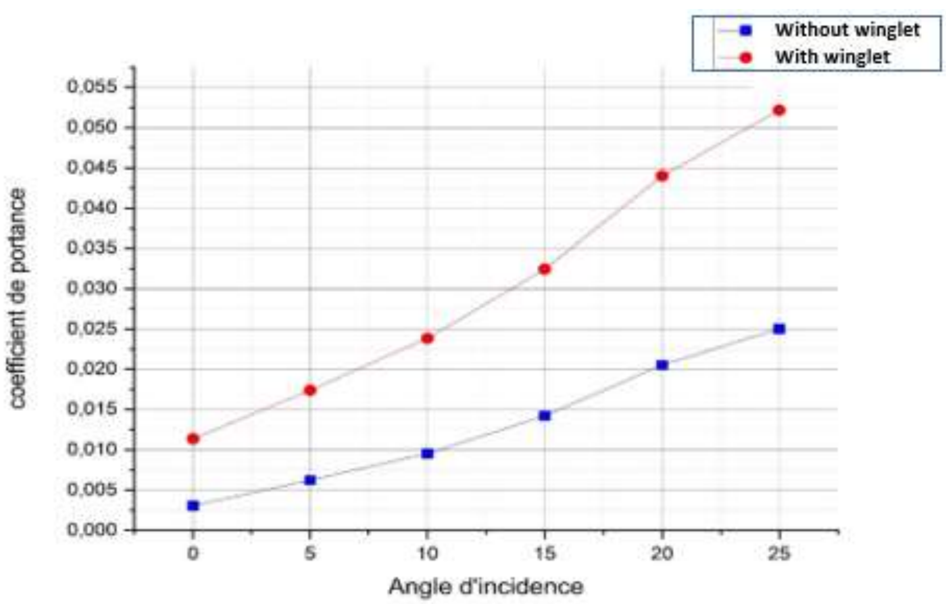

Fig 7: Lift coefficient

Xi'an Shiyou Daxue Xuebao (Ziran Kexue Ban)/
Journal of Xi'an Shiyou University, Natural Sciences Edition
ISSN: 1673-064X
E-Publication: Online Open Access
Vol: 68 Issue 03 | 2025
DOI: 10.5281/zenodo.15112737

This graph (Fig -7-) compares the lift coefficient curves for a wing with and without a winglet across different angles of incidence (angles of attack).

The blue curve represents the lift coefficient for the wing without a winglet, while the red curve shows the lift coefficient with a winglet installed.

At lower angles of incidence up to around 15 degrees, both curves exhibit a fairly linear increase in lift coefficient as the angle increases. However, the slope of the red curve (with winglet) is steeper, indicating a higher lift curve slope and more lift generated per degree angle of attack change compared to the wing without the winglet.

As the angle of incidence increases beyond 15 degrees, the lift curve without the winglet starts to plateau and level off, suggesting the wing is approaching stall. In contrast, the red curve with the winglet continues to rise linearly to higher angles, delaying the stall condition.

Overall, the addition of the winglet results in higher lift coefficients across most angles of attack, with the largest increases observed at higher angles beyond 15 degrees. This enhanced high angle of attack performance can be beneficial during takeoff and landing conditions.

Figure -7- highlights how winglets can improve the aerodynamic efficiency and delay stall compared to a simple wing, enabling higher lift generation, particularly at higher angles of attack encountered during certain flight regimes.

Drag:

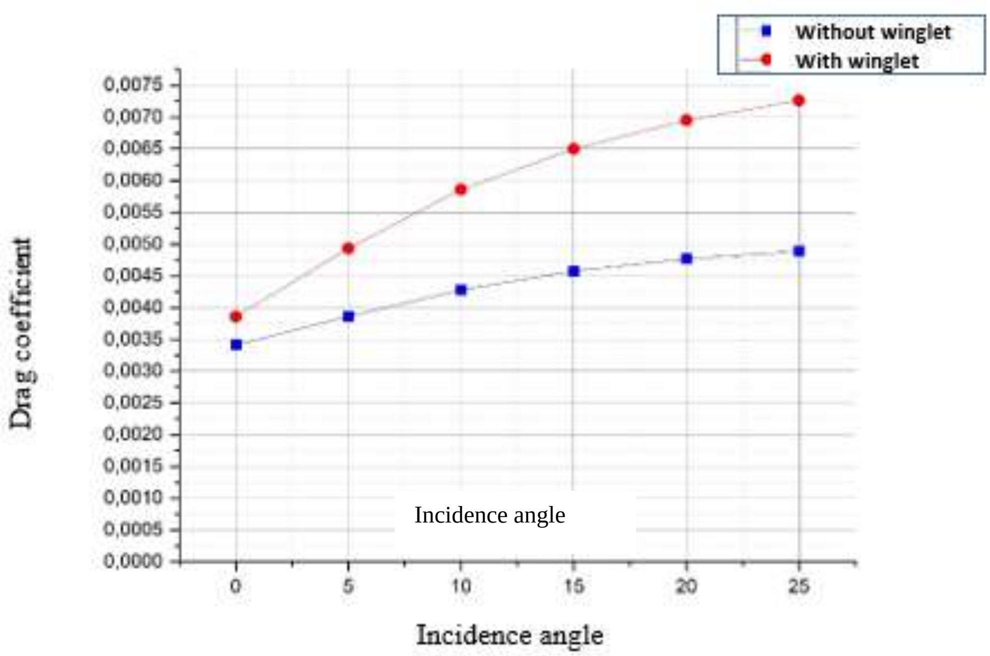

Fig 8: Drag coefficient

Xi'an Shiyou Daxue Xuebao (Ziran Kexue Ban)/
Journal of Xi'an Shiyou University, Natural Sciences Edition
ISSN: 1673-064X
E-Publication: Online Open Access
Vol: 68 Issue 03 | 2025
DOI: 10.5281/zenodo.15112737

Figure 8 compares the drag coefficient curves for a wing with and without a winglet across different angles of incidence (angles of attack). The blue curve represents the drag coefficient for the wing without a winglet, while the red curve shows the drag coefficient with a winglet installed.

At lower angles of incidence up to around 15 degrees, the drag coefficient for the wing without the winglet (blue curve) remains relatively low and almost constant. However, the drag coefficient for the wing with the winglet (red curve) is slightly higher in this low angle of attack range. As the angle of incidence increases beyond 15 degrees, the drag coefficient for the wing without the winglet starts to rise steeply, indicating an increase in drag due to flow separation and stall effects.

In contrast, the drag coefficient for the wing with the winglet (red curve) exhibits a more gradual increase with increasing angle of attack. The winglet appears to delay the onset of significant drag rise associated with stall. At very high angles of attack (beyond around 20 degrees), the red curve shows a more rapid drag increase, but still lower than the wing without the winglet.

Overall, the addition of the winglet results in a slight drag penalty at low angles of attack but offers substantial drag reduction benefits at higher angles, particularly in the post-stall regime. This improved high angle of attack performance can be advantageous during takeoff and landing conditions when the wing operates at higher angles.

While Figure 8 shows a small drag disadvantage for wings with winglets at low speeds (compared to those without), the benefits become substantial at higher angles of attack. Winglets achieve this by delaying the onset of stall, a condition that causes a sharp rise in drag. This delay translates to smoother performance and lower drag at high angles, particularly during takeoff and landing when wings operate at steeper angles. Overall, winglets offer a trade-off: a minor increase in drag at low speeds for a significant reduction in drag at high speeds, leading to improved aerodynamic efficiency.

Comparison of Lift and Drag Coefficients

it plots the lift-to-drag ratio (coef de portance / coef de trainee) against the drag coefficient (coef de trainee) for a wing with and without a winglet.

The black curve represents the wing without a winglet, while the red curve represents the wing with a winglet installed.

At lower drag coefficient values (around 0.0032 to 0.004), both configurations exhibit a relatively linear increase in lift-to-drag ratio as the drag coefficient increases. However, the slope of the red curve (with winglet) is steeper, indicating a more favorable lift-to-drag ratio compared to the wing without the **winglet for a given drag coefficient in this range**

Xi'an Shiyou Daxue Xuebao (Ziran Kexue Ban)/
Journal of Xi'an Shiyou University, Natural Sciences Edition
ISSN: 1673-064X
E-Publication: Online Open Access
Vol: 68 Issue 03 | 2025
DOI: 10.5281/zenodo.15112737

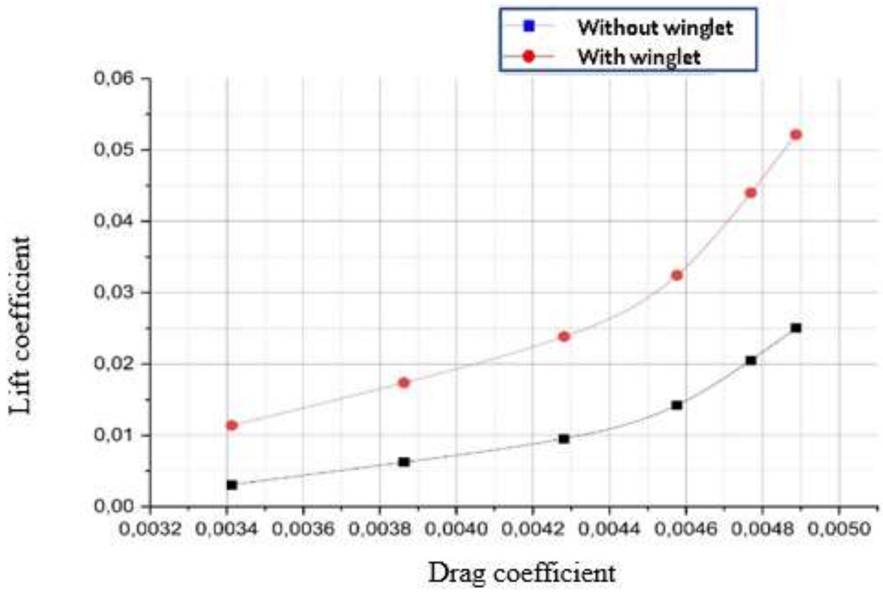

Fig 9: Comparison of Lift and Drag Coefficients

As the drag coefficient continues to increase beyond approximately 0.004, the lift-to-drag ratio for the wing without the winglet (black curve) starts to plateau and level off, indicating a degradation in aerodynamic efficiency as shown in fig -9-. In contrast, the red curve with the winglet maintains a steeper, nearly linear increase in lift-to-drag ratio even at higher drag coefficients. This suggests that the winglet configuration can sustain a higher aerodynamic efficiency (higher lift-to-drag ratio) across a broader range of drag coefficients or flight conditions. The plot effectively illustrates the benefit of the winglet in improving the overall aerodynamic performance by achieving higher lift-to-drag ratios, particularly at higher drag conditions where the plain wing starts to become less efficient. Overall, the graph highlights the winglet's ability to enhance the wing's lift-generating capability relative to the drag penalty, resulting in better aerodynamic efficiency across a wider operational envelope compared to the wing without the winglet.

CONCLUSION

The work presented in this thesis proposes a numerical method to evaluate the lift and drag coefficients, varying the angles of incidence in order to determine which of them is the most efficient. The simulation was carried out with the finite volume calculation code, of which a good number of works validate this approach. The mesh and the control volume were created using a meshing software, then the mesh obtained was exploited by a code to numerically predict the lift and drag coefficients. In this study, the curves that represent the aerodynamic performance are generated as a function of the angles of attack at a speed equal to 20m/s, the study is made for a range of angles of attack between [0°, 25°]

ISSN: 1673-064X
E-Publication: Online Open Access
Vol: 68 Issue 03 | 2025
DOI: 10.5281/zenodo.15112737

On the other hand, we have launched a simulation with the K-ω SST turbulence model (known for its good capture of separated flows) in order to see the improvement that this model can bring. Although it brings a certain improvement, it is also unable to capture the stall phenomenon. Based on the analysis of the lift coefficient and drag coefficient curves presented in these graphs, the following detailed conclusions can be drawn from this study:

Lift Coefficient Characteristics:

The wing with the spiroid winglet (red curve) exhibits a higher lift coefficient slope at lower angles of attack compared to the wing without the winglet (blue curve). The winglet delays the onset of flow separation and stall, allowing the wing to maintain higher lift coefficients at higher angles of attack beyond 15 degrees. The improved high-angle-of-attack performance of the winglet-equipped wing can be beneficial during critical flight phases like takeoff and landing.

Drag Coefficient Characteristics:

At low angles of attack, the wing with the winglet experiences a minor increase in drag coefficient compared to the wing without the winglet. As the angle of attack increases, the drag coefficient rise for the wing without the winglet becomes much steeper, indicating a more rapid onset of flow separation and stall. In contrast, the winglet-equipped wing exhibits a more gradual increase in drag coefficient with angle of attack, delaying the drag rise associated with stall. The winglet's ability to suppress drag rise at high angles of attack can enhance the wing's aerodynamic efficiency during off-design conditions.

Lift-to-Drag Ratio Performance:

The graph comparing lift-to-drag ratio against drag coefficient shows that the winglet-equipped wing achieves a significantly higher lift-to-drag ratio across a wider range of drag coefficients. The steeper slope of the lift-to-drag ratio curve for the winglet configuration indicates superior aerodynamic efficiency compared to the wing without the winglet. This improvement in the overall lift-to-drag ratio can translate to tangible benefits in terms of increased aircraft performance, reduced fuel consumption, and enhanced operational capabilities. In conclusion, the incorporation of a spiroid winglet on the wing has demonstrated substantial improvements in the aerodynamic characteristics, including increased lift coefficients, delayed stall, reduced drag rise, and enhanced lift-to-drag ratio performance. These findings highlight the potential of the spiroid winglet design to enhance the overall efficiency and operational capabilities of aircraft wings compared to a conventional wing without a winglet.

Data Availability Statement:

The data that support the findings of this study are not available due to privacy restrictions. Further inquiries regarding data availability should be directed to the corresponding author.

Competing Interest Declaration: No

Ethical Statement:

This study was conducted in accordance with ethical guidelines and principles. All procedures involving human participants were in compliance with the ethical standards of the institutional and/or national research committee. Informed consent was obtained from all individual participants included in the study. Participants were made aware of their right to withdraw from the study at any time without consequence. All data collected were treated confidentially and anonymized to protect participant privacy.

Funding Declaration: No

Author Contribution Statement:

- Zineb HEMMAMI.: Conceptualization, - original draft. Data curation, Software, Visualization, Validation.
- Azzeddine HAMMAMI.: Methodology, Formal analysis, Investigation, WritingWriting - review & editing.

All authors have read and agreed to the published version of the manuscript.

Bibliography

1) Guerrero, J. E., Maestri, D., & Bottaro, A. (2012). Biomimetic spiroid winglets for lift and drag control. Comptes Rendus Mecanique, 340(4-5), 425-432.

2) Ning, S. A., & Kroo, I. (2010). Integrated design exploration of spiroid winglets for wing drag reduction. AIAA Paper, 5033, 2010.

3) Bourdin, P., Gatto, A., & Friswell, M. I. (2007). Aircraft wing aerodynamic model with curved-planform spiroid winglet. Journal of Aircraft, 44(4), 1121-1130.

4) Takenaka, K., Hatanaka, K., Wheeler, A. P., & Goldey, C. L. (2008). Aerodynamic performance of NACA 2412 wing at Low-Reynolds numbers. AIAA paper, 442.

5) Maughmer, M. D. (2003). Design study of spiroid winglets for wing-induced drag reduction. AIAA paper, 147.

6) Najafian Ashraf, Z., & Sedaghat, A. (n.d.). Improving the Aerodynamic Performance of a Wing with Winglet [Abstract]. ResearchGate. Retrieved March 30, 2024, from

7) Hui, Z., Cheng, G., & Chen, G. (2021). A Brief Review on Aerodynamic Performance of Wingtip Slots and Research Prospect. Journal of Bionic Engineering, 1-12.

8) Nicolosi, F., Scherillo, F., Maisto, U., & Coiro, D. P. (2021). Aerodynamic Efficiency Study of Modern Spiroid Winglets. In A. Zingoni (Ed.), ICAS Proceedings 2006 (Vol. 14, pp. 899–908).

9) Mostafa, Suhail, et al. « A parametric investigation of non-circular spiroid winglets ». EPJ Web of Conferences, édité par Tomáš Vít et al., vol. 67, 2014, p. 02077. DOI.org (Crossref), https://doi.org/10.1051/epjconf/20146702077.

10) Fathi, Behrouz. « Applying Spiroid Winglet on The Tip of NREL 5 MW Offshore Wind Turbine's Blade to Investigate Vortex Effects ». E3S Web of Conferences, édité par ATI Associazione Termotecnica Italiana, vol. 197, 2020, p. 08004. DOI.org (Crossref), https://doi.org/10.1051/e3sconf/202019708004.

11) Dhileep, Karthick, et al. « Aerodynamic Characteristics of Semi-spiroid Winglets at Subsonic Speed ». Innovative Design, Analysis and Development Practices in Aerospace and Automotive Engineering (I-DAD 2018), édité par U. Chandrasekhar et al., Springer Singapore, 2019, p. 217-24. DOI.org (Crossref), https://doi.org/10.1007/978-981-13-2718-6_20.

12) Matsson, J.E., Voth, J.A., McCain, C.A. and McGraw, C. (2016), "Aerodynamic performance of the NACA2412 airfoil at low reynolds number", 2016 ASEE Annual Conference & Exposition, New Orleans, Louisiana, June.